New Reduced-Size Step-Impedance Dual-Band Filters with Enhanced Bandwidth and Stopband Performance

Marjan Mokhtaari[1], Jens Bornemann[1] and Smain Amari[2]

[1] University of Victoria, Victoria, BC, Canada V8W 3P6
[2] Royal Military College of Canada, Kingston, ON, Canada K7K 7B4

ABSTRACT — **This paper presents new configurations for dual-band filter designs. Stepped impedance resonators are used to implement the dual-band characteristics. Due to their tunable spurious response properties, the new filters feature two controllable passbands at desired frequencies, high out-of-band rejection as well as a wide stopband regions created by a zero-phase feed structure without input/output matching networks. Moreover, the new topologies occupy less circuit space in comparison with traditional designs. Several new dual-band filter configurations have been designed on RT-Duroid 6006 substrate. Performances are verified using commercially available field solvers.**

Index Terms **— Filter design; stepped impedance resonators; dual-band filters; microstrip filters.**

I. INTRODUCTION

Dual-band filters emerged mostly due to the broad demand for multiple frequency bands in wireless communication applications, e.g. [1-4]. They were usually implemented by combining and switching two separate filters operating over two different frequency bands [1]. These architectures increase size, cost, efficiency and power dissipation by a factor of two compared to single bandpass filters. Alternatively, shunt stubs are used to create transmission zeros in order to separate the passbands and increase the stopband region [3-4]. A concurrent dual-band filter integrates the characteristics of each passband filter in a single circuit, which generates two passbands located at two desired frequencies without introducing additional losses or a significant increase in cost and size.

Due to their tunable harmonic response property, step-impedance resonators (SIR's) [5-7] generate the highly selective dual-band effect. The inter-resonator coupling coefficients play an essential role in the design of dual-band filters and are distinctly different from those in classical bandpass filters. Therefore, the achievable values of coupling coefficients and percentage bandwidth are limited in traditional coupling schemes (Fig. 1) when operated at two separated passbands.

The purpose of this paper is to introduce new coupling configurations with SIR's (Fig. 2), which provide controllable dual-band filter characteristics. The bandwidths and quality factors are controlled by the electric coupling at the ends of the transmission lines and by a zero-phase feed structure at both pass-bands. The latter permits creation of transmission zeros on each side of the passbands to generate high levels and wide stopband regions. Therefore, the new dual-band filter configurations are free of any input and output step-impedance transformers.

As examples, several dual-band filters are designed and simulated. By appropriately adjusting the impedance ratios, the second passband can occur at one to two times the first passband frequency. Moreover, a comparison is presented between dual-band filter schemes, which differ in tunable bandwidths, number of transmission zeros, stop-band region characteristics as well as total size.

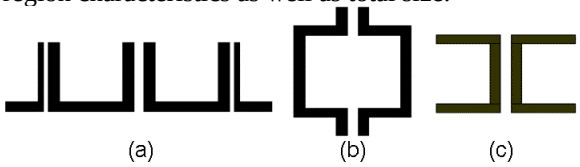

Fig. 1. Some traditional dual-band coupling schemes: (a) comb-line, (b) end-coupled, (c) transmission-line coupler.

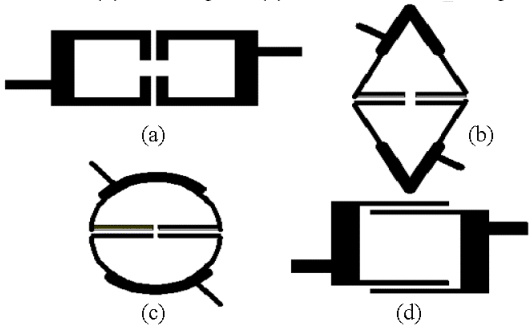

Fig. 2. New dual-band coupling configurations: (a) new end-coupled, (b) triangular, (c) circular, (d) new hairpin.

II. DESIGN

Fig. 3 shows the basic structure of a half wavelength SIR. Z_1 and Z_2 are the characteristics

0-7803-9542-5/06/$20.00 ©2006 IEEE

impedances of the transmission line sections whose electrical lengths are θ_1 and θ_2, respectively. The resonance condition can be analyzed by deriving the input admittance viewed from an open end

$$Y_{in} = \frac{j2Y_2(K\tan(\frac{\theta_1}{2})+\tan\theta_2)(K-\tan(\frac{\theta_1}{2})\tan\theta_2)}{K(1-\tan^2\frac{\theta_1}{2})(1-\tan^2\theta_2)-2(1-K^2)\tan(\frac{\theta_1}{2})\tan\theta_2} \quad (1)$$

where $K=Z_2/Z_1$. The fundamental and second harmonic resonance frequencies f_1, f_2 with corresponding electrical lengths θ_{s1} and θ_{s2}, respectively, are calculated through odd- and even-mode resonance conditions [5]

$$\begin{aligned} K &= \tan(\frac{\theta_1}{2})\tan(\theta 2) \quad \Rightarrow f_1 \\ K\tan(\frac{\theta_1}{2}) &= -\tan(\theta 2) \quad \Rightarrow f_2 \end{aligned} \quad (2)$$

The ratio of resonance frequencies depends on K [5] such that

$$\begin{aligned} f_2/f_1 &< 2 \quad if \quad K > 1 \\ f_2/f_1 &= 2 \quad if \quad K = 1 \\ f_2/f_1 &> 2 \quad if \quad K < 1 \end{aligned} \quad (3)$$

These conditions are utilized to design dual-band filters with different frequency ratios. In the special case where $\theta_1=2\theta_2$, (2) simplifies to

$$\theta_{s1} = \tan^{-1}(\sqrt{K}), \quad \theta_{s2} = \pi/2 \quad (4)$$

The main dual-band filter design function relating the ratio of both resonance frequencies is defined as:

$$\frac{\theta_{s1}}{\theta_{s2}} = \frac{f_2}{f_1} = \frac{\pi}{2\tan^{-1}(\sqrt{K})} \quad (5)$$

This implies that by appropriately determining the impedance ratio K, two pass-bands with any desired frequency ratio are achieved [6].

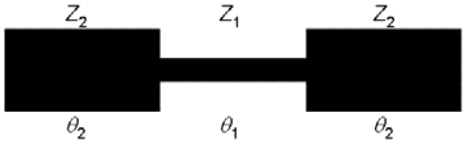

Fig. 3. Basic structure of half-wavelength SIR.

The next step in the design process is the determination of proper topologies to realize the coupling between step-impedance resonators, which is crucial for the bandwidth control of dual-band filters. Fig. 1 shows the conventional coupling schemes. At the fundamental resonance frequency, the step-impedance resonator has strong electric and magnetic couplings at both ends and at the center of the transmission lines, respectively. At the first harmonic resonance frequency, the magnetic coupling at the center converts to electrical coupling – due to the reduction in wavelength - thus changing the coupling coefficient for the second pass-band completely and making independent tuning impossible.

Therefore, an appropriate choice for dual-band filters is to utilize the inter-coupled open-ends of transmission-line resonators (c.f. Fig. 2a-2d).

For a half wavelength resonator, there are two proper feed points at opposite locations slightly off the center of the resonator. Fig. 4 shows two electric coupling structures constructed by hairpin resonators with different input feed points.

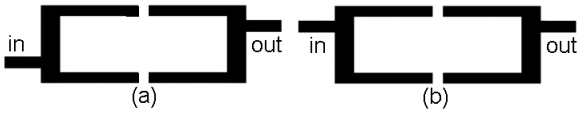

Fig. 4. In-phase (a) and out-of-phase (b) feed structures.

In Fig. 4a, the input and output feed points are in phase when the circuit resonates at its fundamental frequency, whereas in Fig. 4b they are out of phase. Both arrangements can be used to design a filter. However, the configuration in Fig. 4a creates two more attenuation poles [8]. By slightly adjusting the actual feed locations and couplings in Fig. 4a, one attenuation pole can be located in the lower and one in the upper part of the stopband region. In a folded arrangement of two hairpin step-impedance resonators (similar to Fig. 1a), possible cross coupling between input and output creates the potential for two additional poles in the stopband. In summary, a number of additional attenuation poles increase the out-of-band rejection and thus the applicable frequency range of these filters. Note that the new dual-band filter schemes are usually smaller in comparison with the traditional ones and that they do not require input/output impedance matching networks.

Figs. 2a-2c show three different dual-band filter configurations with folded rectangular, triangular and circular step-impedance resonators, respectively. These new dual-band filter structures have a similar structure as that in Fig. 1b, but smaller size, larger bandwidth and broad out-of-band rejection. The tapered in-phase input/output feed points used in these configurations do not require impedance matching as is essential for the structure in Fig. 1b.

The last new dual-band filter configuration shown in Fig. 2d is a complement of Fig. 1c with electric coupling at the end rather than magnetic coupling at the center. It has the same input/output feed point as the previous filter structure, thus creating additional transmission zeros. It also has smaller dimension, more flexible bandwidth control and a wider stopband region than that in Fig. 1c.

III. Results

This section presents typical performance characteristics for the new dual-band filter configurations. All dual-band pass-band filters have been designed on RT-DUROID 6006 substrate, with 1oz metal thickness and 0.64mm substrate height.

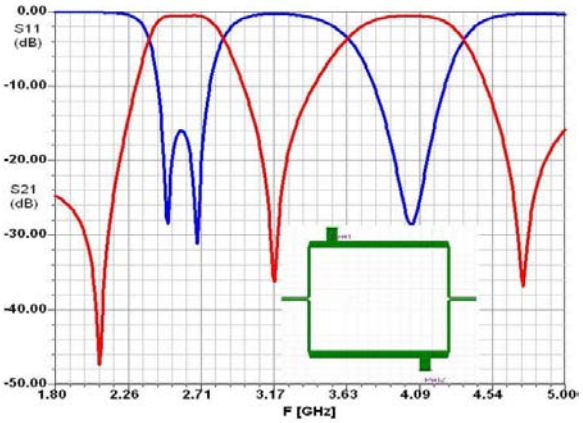

(a)

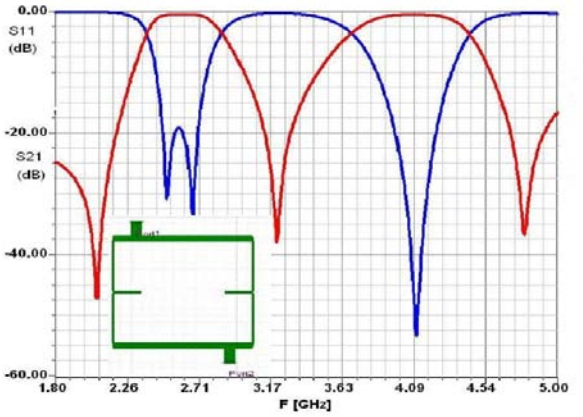

(b)

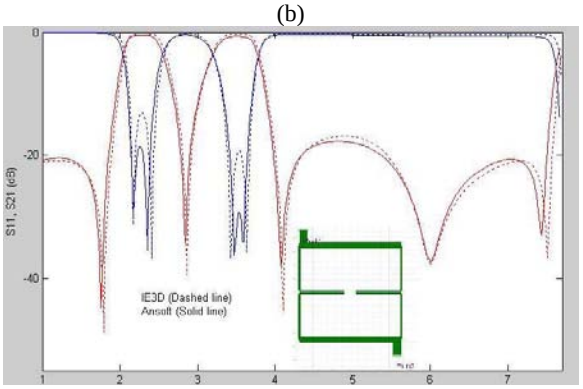

(c)

Fig. 5. Filter performances of conventional dual-band configuration (a, b) and the new square open-loop (new end-coupled) dual-band configuration (c).

Fig. 5 shows a performance comparison between conventional step-impedance filters (Figs. 5a, 5b) and the new design (Fig. 5c) implemented by compact rectangular open-loop resonators according to Fig. 2a. The new configuration in Fig. 5c demonstrates larger bandwidths (250 MHz in each pass-band compared to 200MHz in Figs. 5a and 5b, higher selectivity and smaller size with the same step-impedance resonator characteristics. Moreover, the results of the new dual-band resonators in Fig. 5c illustrate the flexibility of the new topology to obtain closer passbands, more bandwidth and a clean stopband up to the next possible harmonic frequency.

The next two examples, shown in Fig. 6 and Fig. 7, are two step-impedance dual-band filters designed by using the triangular and circular configurations in Figs. 2b and 2c. The center frequencies are at 2 and 3 GHz with 150MHz bandwidth in each pass-band for the triangular configuration and 2.2 and 3.3GHz with 170MHz bandwidth for the circular configuration The transmission zeros are located at 1.6GHz, 2.4GHz and 3.4GHz for the triangular structure and 1.7GHz, 2.75GHz and 3.8GHz for the circular configuration. One of the advantages of these new configurations is that they are versatile and have smaller size and wider bandwidths than the classical schemes. Both filters demonstrate similar performances. But the circular configuration in Fig. 7 achieves better return loss at the expense of slightly reduced stopband attenuation.

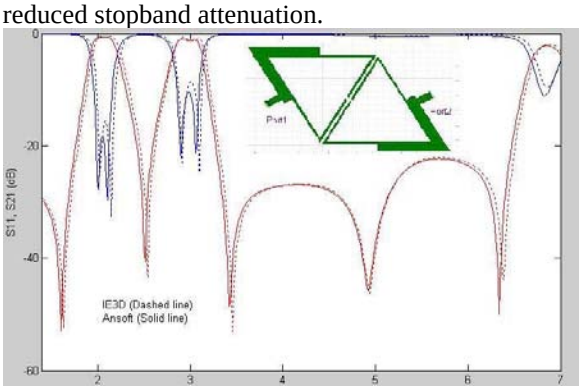

Fig. 6. Response (versus frequency in GHz) of the new triangular dual-band configuration according to Fig. 2b.

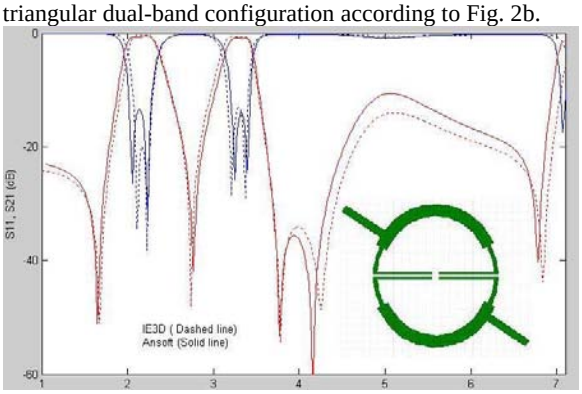

Fig. 7. Response (versus frequency in GHz) of the new circular dual-band configuration according to Fig. 2c.

The new scheme of end-coupled hairpin resonators (Fig. 2d) is used to design a dual-band filter with center frequencies at 2.25GHz and 3.55GHz and 400MHz bandwidth in each passband. Fig. 8 presents the filter characteristic. The transmission zeros are located at 1.6 GHz, 2.5 GHz and 3.5 GHz.

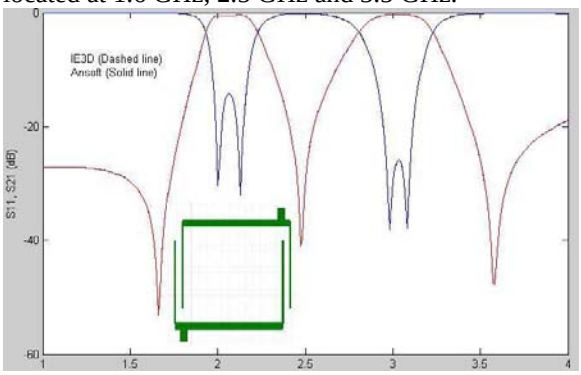

Fig. 8. Response (versus frequency in GHz) of the new dual-band hairpin configuration according to Fig. 2d. (Note that the two sets of curves are identical to within the plotting accuracy.)

Higher order dual-band filter designs with wider bandwidths can be completed by cascading *N* dual-band configurations to create 2*N*-1 reflection zeros in each pass-band. In this case, the locations and number of transmission zeros are the same as those for one stage; however, their stopband attenuation increases with the number of stages.

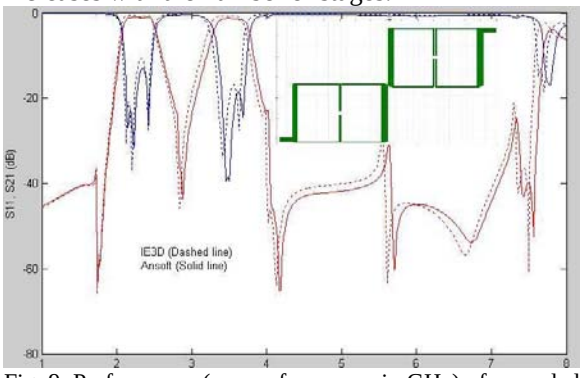

Fig. 9. Performance (versus frequency in GHz) of cascaded new end-coupled dual-band filter using two single square-open loop dual-band configurations.

Fig. 9 shows two cascaded dual-band filters including three reflection zeros in each band (the return loss dip in the upper band contains two zeros). The center frequencies are 2.3 GHz and 3.5 GHz; the bandwidths are approximately 400 MHz. Note that the bandwidth is almost doubled compared to that of the single configuration in Fig. 5c.

IV. Conclusions

This paper presents a number of new dual-band filter designs based on step-impedance resonators. The frequency responses are comparable to those of conventional dual-band filters but exhibit one or two additional transmission zeros on each side of the central bandwidth, thus increasing out-of-band rejection. Cascaded versions of the new single dual-band configurations can be used to create higher order dual-band filters with wider bandwidths. In addition, due to their compressed structure without matching networks, the new designs require less circuit-board space.

References

[1] H. Miyake, S. Kitazawa, T. Ishizaki, T. Yamada, Y. Nagatomi, "A miniturized monolithic dual band filter using ceramic lamination technique for dual mode portable telephones", IEEE MTT-S Int. Microwave Symp. Dig., pp. 789-792, Denver, CO, June 1997.

[2] S. Avrillon, A. Chousseaud, S. Toutain, "Dividing and filtering function integration for the development of a band-pass filtering power amplifier", IEEE MTT-S Int. Microwave Symp. Dig., pp. 1173-1176, Seattle, WA, June 2002.

[3] C. Quendo, E. Rius, C. Person, "Narrow bandpass filters using dual-behavior resonators", IEEE Trans. Microwave Theory Tech., Vol. 51, pp. 734-743, Mar. 2003.

[4] C. Quendo, E. Rius, C. Person, "Narrow bandpass filters using dual-behavior resonators based on stepped-impedance stubs and different-length stubs", IEEE Trans. Microwave Theory Tech., Vol. 53, pp. 1034-1044, Mar. 2004.

[5] H.-M. Lee, C.-R. Chen, C.-C. Tsai, C.-M. Tsai, "Dual-band coupling and feed structure for microstrip filter design", IEEE MTT-S Int. Microwave Symp. Dig., pp. 1971-1974, Fort Worth, TX, June 2004.

[6] A.A.A. Apriyana, Z.Y. Ping, **"**A dual-band BPF for concurrent dual-band wireless transceiver**",** Proc. 5th Electronics Packaging Technology Conference (EPTC), pp. 145 – 149, Dec. 2003.

[7] S.-F. Chang, Y.-H. Jeng, J.-L. Chen, "Dual-band step-impedance bandpass filter for multimode wireless LANs", Electronics Letters, Vol. 40, pp. 38-39, Jan. 2004.

[8] S.-Y. Lee, C.-M. Tsai, "New cross-coupled filter design using improved hairpin resonators", IEEE Trans. Microwave Theory Tech., Vol. 48, pp. 2482-2490, Dec. 2000.